

ference extends to dilute alloys. The possibility that the transition temperatures observed in the present work were too high owing to the "quench effect"^{16,17} seems unlikely since the samples were annealed for some days at room temperature before measuring.

CONCLUSION

The absence of a resistance minimum and the saturation of superconducting-transition-temperature depression with increasing impurity concentration are reasons for doubting whether manganese dissolved in indium does have a localized magnetic moment. However, the

¹⁶ M. F. Merriam and M. A. Jensen, *Cryogenics* **2**, 301 (1962).
¹⁷ M. F. Merriam and M. von Herzen, *Phys. Rev.* **131**, 637 (1963).

initial rate of depression of transition temperature with increasing residual-resistivity ratio is unusually high.

[*Note added in proof.* F. T. Hedgcock and W. B. Muir, *Phys. Letters* **14**, 11 (1965), have recently published the results of magnetoresistance measurements on some of the In-Mn alloys made by Merriam *et al.*⁹ These results support the conclusion reached in the present paper that localized magnetic moments in In-Mn are unlikely.]

ACKNOWLEDGMENTS

I am indebted to Professor B. Serin for commenting on the manuscript, to W. Fisher for making the alloys, to D. S. Russell for the spectrographic analysis and to R. L. Snowdon for assistance with the experiments.

Localized Moments Associated with Very Dilute Fe Impurities in Some Transition and Noble Metals*

T. A. KITCHENS, W. A. STEYERT, AND R. D. TAYLOR

University of California, Los Alamos Scientific Laboratory, Los Alamos, New Mexico

(Received 23 November 1964)

The magnetic behavior of very dilute (<0.1%) iron impurities in Cu, Ag, Au, V, Nb, Ta, Mo, W, Rh, and Pt has been studied by the Mössbauer effect in Fe⁵⁷ for applied fields to 62 kOe and temperatures from 0.5 to 300°K. For V, Nb, and Ta the hyperfine field at the impurity nucleus corresponds directly to the applied field to within 1.5 kOe; no localized moment exists. For the other metals, an internal field is found which is antiparallel to the applied field. The functional behavior of the internal fields is analyzed in terms of localized magnetic states associated with the Fe impurities, which do not interact with one another, but are not, in general, completely free. The localized magnetic moments, which range to 6.0 μ_B , can be correlated with the average concentration of electrons outside the last full shell, and agree with the moments derived from available magnetic-susceptibility measurements. Temperature and chemical shifts for these sources are given.

INTRODUCTION

RECENTLY it has been shown¹ by Mössbauer-effect measurements on very dilute Fe in Pd that the dependence of the internal field H_i on the temperature T and the applied field H yields giant localized moments on the Fe, in good agreement with the results from susceptibility measurements.^{2,3} Clogston *et al.*² reported on a number of alloys of the second-row transition metals containing 1% Fe and found a good correlation between the magnitude of a localized moment and the electron concentration n , the average number of electrons outside the last closed shell of the host alloy. The applicability of this correlation to the

third-row transition metals has been confirmed for Fe in Pt.¹

The nature of a localized state confined to an impurity for a metallic host has been extensively treated by Friedel.⁴ The problem has also been considered by Anderson,⁵ Wolff,⁶ Suhl and Fredkin,⁷ and Clogston⁸ with particular emphasis on application to the susceptibility results. Marshall *et al.*⁹ have considered the particular case of the Mössbauer effect of Fe⁵⁷ in dilute alloys generally with regard to higher concentrations in ferromagnetic systems with no external field.

The Mössbauer effect is useful in the study of the magnetic behavior of dilute Fe impurities because (1)

* Work performed under the auspices of the U. S. Atomic Energy Commission.

¹ P. P. Craig, D. E. Nagle, W. A. Steyert, and R. D. Taylor, *Phys. Rev. Letters* **9**, 12 (1962).

² A. M. Clogston, B. T. Matthias, M. Peter, H. J. Williams, E. Corenzwit, and R. C. Sherwood, *Phys. Rev.* **125**, 541 (1962).

³ D. Gerstenberg, *Ann. Physik* **2**, 236 (1958); J. Crangle, *Phil. Mag.* **5**, 335 (1960); R. M. Bozorth, P. A. Wolff, D. D. Davis, V. B. Compton, and J. H. Wernick, *Phys. Rev.* **122**, 1157 (1961).

⁴ J. Friedel, *Nuovo Cimento Suppl.* **7**, 287 (1958); also A. Blandin and J. Friedel, *J. Phys. Radium* **20**, 160 (1959).

⁵ P. W. Anderson, *Phys. Rev.* **124**, 41 (1961).

⁶ P. A. Wolff, *Phys. Rev.* **124**, 1030 (1961).

⁷ H. Suhl and D. R. Fredkin, *Phys. Rev.* **131**, 1063 (1963).

⁸ A. M. Clogston, *Phys. Rev.* **125**, 439 (1962).

⁹ W. Marshall, T. E. Cranshaw, C. E. Johnson, and M. S. Ridout, *Rev. Mod. Phys.* **36**, 399 (1964); W. Marshall and C. Johnson, *J. Phys. Radium* **23**, 733 (1962).

useful measurements are possible with concentrations low enough that impurity-impurity interactions are surely negligible, and (2) the isotope Fe^{57} exhibits an appreciable resonance even at room temperature, has a known nuclear magnetic moment, and has a convenient long-lived parent Co^{57} . In the presence of sufficient magnetic field Fe^{57} has a clearly resolvable nuclear hyperfine spectrum; the effective field H_{eff} may readily be deduced from the observed splitting. H_{eff} is the sum of the applied field H (the direct interaction of H on the Fe^{57} nuclear moment) and an internal field H_i which arises principally from polarization of the s electrons by the d electrons of the Fe atom; H_i is assumed to be directly proportional to the magnetization.^{1,10,11}

In general, one obtains the following from these measurements: μ , the localized moment on the Fe impurity; J , the spin associated with the Fe; H_{sat} , the value of H_i for a fully aligned moment; and a parameter s deduced from the observed deviations from free-spin behavior.^{12,13} Except for Fe in Au, no dependence on magnetic impurity concentration has been found.

In addition to the magnetic results, a crude measure of the effective θ_{Debye} for Fe^{57} in the various host materials is obtained from the shift of the Mössbauer spectrum as a function of temperature.¹⁴ A relative measure of $|\psi(0)|^2$, the electron density at the Fe nucleus, is obtained by comparing the shifts between various sources at a given high temperature.¹⁵

Preliminary data on some of the same host materials reported here have been presented elsewhere.^{12,16,17} Blum *et al.*¹⁸ have made similar Mössbauer studies generally using alloy absorbers containing 1% Fe^{57} .

APPARATUS

Cryostat

The He^4 cryostat used in this research was not unusual; however, several of its features, particularly those associated with the temperature control of the source, warrant discussion. A 0.505-in. i.d., 60-kOe Nb-Zr superconducting solenoid (Westinghouse Electric Corporation) in the bottom of the He^4 pot was located on axis by a 0.5-in. o.d., 0.008-in. wall German-silver tube soldered at the bottom. This tube extended up

through the magnet and through the top of the cryostat and served as a vacuum jacket for the sources to be studied; the sources were placed in the center of the magnet on a holder on the end of a long 0.375-in. o.d. Inconel tube. Vertical and axial alignment was obtained by a copper taper on the smaller tube, which fitted a matching female taper soldered inside the 0.5-in. tube. The taper, located about 7 in. above the center of the magnet, also served as a thermal short between the inner tube and the He^4 bath; slots allowed gas flow through the taper. A specially prepared Be window¹⁹ was soft soldered to the bottom of the 0.5-in. tube to allow the use of exchange gas in the annulus without destroying the main Dewar vacuum. An aluminized Mylar window on the N_2 shield and 0.020-in.-thick Be window at room temperature allowed passage of the γ rays out the bottom of the cryostat.

A threaded collar held the flat disk sources on the bottom end of the source holder. A film of Apiezon N grease was applied to improve the thermal contact. A 0.150-in.-diam portion of the holder extended up about 2 in. into the Inconel tube. Attached to this pedestal were two calibrated carbon resistance thermometers, a copper-constantan thermocouple, a manganin heater, and the necessary electrical leads. The Inconel tube could be evacuated or filled with exchange gas. In the latter case the heat transfer between the holder and the copper taper could be varied²⁰ by a 7-in.-long thin-walled copper tube whose height could be adjusted. By proper control of the bath temperature, the exchange gas, the heater current, and the shunt tube height, the source could be maintained at any temperature between 1.1 and 300°K. That the sample thermal contact was adequate was proved by the fact that the same results were obtained at low T with and without exchange gas and by the fact that the same temperature shift obtained at 298°K before cooldown was obtained with the magnet at 4°K and the source (holder) maintained at 298°K by the electrical heater. The resistance thermometers and thermocouple were calibrated *in situ* by filling the He^4 pot with N_2 and H_2 and He^4 at various vapor pressures (temperatures) with the annulus surrounding the source holder filled with He^4 exchange gas. The vapor pressure of a small amount of He^4 or $n\text{-H}_2$ condensed in the 0.375-in. tube indicated the sample holder indeed to be at the bath temperature. Graphical interpolation of the resistance at intermediate temperatures gave T to better than 1%. Above 100°K, the thermocouple was used.

A separate source-holder assembly allowed the use of liquid He^3 to obtain source temperatures as low as 0.42°K in the solenoid. Temperatures were determined from the vapor pressure of the He^3 . The current in the solenoid was measured to better than 0.1%, and was then made persistent for the actual measurements.

¹⁰ D. E. Nagle, H. Frauenfelder, R. D. Taylor, D. R. F. Cochran, and B. T. Matthias, *Phys. Rev. Letters* **5**, 364 (1960).

¹¹ R. E. Watson and A. J. Freeman, *Phys. Rev.* **123**, 2027 (1961).

¹² R. D. Taylor, T. A. Kitchens, D. E. Nagle, W. A. Steyert, and W. E. Millett, *Solid State Commun.* **2**, 209 (1964).

¹³ R. M. Housley and J. G. Dash, *Rev. Mod. Phys.* **36**, 409 (1964); *Phys. Letters* **10**, 270 (1964).

¹⁴ R. V. Pound and G. A. Rebka, *Phys. Rev. Letters* **4**, 274 (1960).

¹⁵ L. R. Walker, G. K. Wertheim, and V. Jaccarino, *Phys. Rev. Letters* **6**, 98 (1961).

¹⁶ R. D. Taylor, W. A. Steyert, and D. E. Nagle, *Rev. Mod. Phys.* **36**, 406 (1964).

¹⁷ R. D. Taylor, T. A. Kitchens, and W. A. Steyert, *Proceedings of Ninth International Conference on Low Temperature Physics*, Columbus, Ohio (to be published).

¹⁸ N. Blum, A. J. Freeman, and L. Grodzins, *Rev. Mod. Phys.* **36**, 406 (1964).

¹⁹ R. D. Taylor, W. A. Steyert, and A. G. Fox, *Rev. Sci. Instr.* (to be published).

²⁰ J. G. Dash and J. Siegwarth, *Rev. Sci. Instr.* **34**, 1276 (1963).

Spectrometer

A schematic of the Mössbauer spectrometer is shown in Fig. 1. In all the work reported here the 14.4-keV Fe^{57} γ rays from the source were analyzed by a Doppler-shifted room-temperature absorber. The Doppler shifting device consists of the ring magnet assemblies from two loudspeakers mounted back to back. A hole drilled axially accepts a 1-in.-diam thin-walled Inconel tube. Two loudspeaker spiders locate the two 1.5-in.-diam voice coils, which are mechanically coupled via the tube and a pair of bushing adapters. The motion of the absorber, which is attached to the tube, is produced by the upper speaker and is detected by the lower speaker. As shown, a feedback circuit produces a velocity waveform at the absorber which is the same as that produced by the function generator. For a velocity changing linearly with time a good waveform is obtained up to maximum velocities of about 12 mm/sec at frequencies as low as 6 cps. A multichannel analyzer (RIDL-Model 34-12B) operating in the "time mode" is used to store the number of 14.4-keV counts received through the absorber during 400 equal time intervals for each cycle of the function generator. This is accomplished by using the synchronizing pulse (occurring once each cycle in the function generator, Hewlett-Packard 202A) to start a chain of pulses from the crystal-controlled time-base generator (RIDL-Model 54-6), which, in our case, advances the channel every 400 μsec ; an address overflow pulse at the end of 400 channels stops the channel advance pulses; then the cycle is repeated. Thus, each channel corresponds to a given relative velocity of the absorber. The first 200 channels are used to store from, say, $-v_{\text{max}}$ to $+v_{\text{max}}$, whereas the second 200 channels are used for the other half-cycle from $+v_{\text{max}}$ to $-v_{\text{max}}$. Such a system has several advantages over other multichannel systems. The display is an undistorted counts versus velocity Mössbauer spectrum (since the counting time and small dead time are the same in each channel and the drive is linear), and small nonlinearities of the drive are compensated for by averaging the results from the two halves of the memory.

A xenon-filled proportional counter (Reuter Stokes, RSG-30A) was used to detect the γ rays. Its high resolution is desirable in order to be able to reject the nearby x rays present in several of the sources used. Such discrimination is accomplished using a single-channel analyzer.

Absorbers

An enriched $\text{K}_4\text{Fe}(\text{CN})_6 \cdot 3\text{H}_2\text{O}$ absorber was used in essentially all of the work reported here. It was prepared by dipping a disk of filter paper into a solution of the salt and allowing it to dry. An annealed, enriched Fe absorber containing 0.8 mg $\text{Fe}^{57}/\text{cm}^2$ was used for calibration purposes.

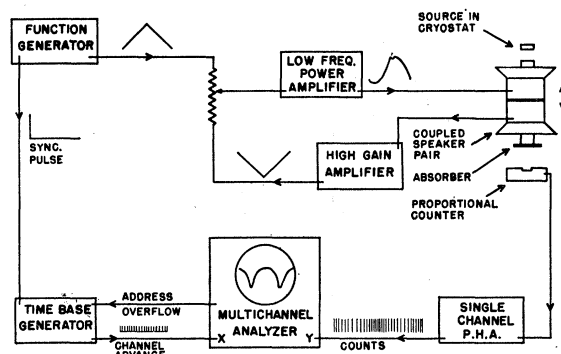


FIG. 1. A schematic drawing of the Mössbauer spectrometer.

SOURCES

These experiments were designed to study the nature of the impurity state in the absence of the complicating, but interesting, effects of impurity-impurity interactions. As shown in Table I most starting materials were analyzed spectroscopically and have less than 100-ppm magnetic impurities. The host metals were in the form of 0.340-in.-diam disks 0.005 to 0.025 in. thick. In addition a 0.00014-in.-thick gold foil source was used. The quality of the single crystals was checked by x-ray diffraction before annealing (and after annealing for the Au and Ag crystals).

Each lot of "high-purity, carrier-free" $\text{Co}^{57}\text{Cl}_2$ radioactive solution was spot tested for the presence of Fe, Co, or Ni and estimates, noted in Table I, were made of the total μg (micrograms) of Fe, Co, and Ni per mCi.²¹ Pure Co^{57} would give 0.12 $\mu\text{g}/\text{mCi}$.

The activity was then dried from solution onto the host metal and was counted in a standard counter geometry to measure N_{14}^0 , the 14.4-keV, and N_{123}^0 , the 123-keV, counting rates before annealing. Then the source was reduced with H_2 and diffusion annealed as shown in Table I, and in most cases washed, or etched. (A tungsten-tube furnace was used for all annealing above 1400°C. Below 1220°C, a quartz-tube furnace with a nichrome heater was used.) The source was recounted in the standard geometry and from the loss in the 14.4-keV γ rays relative to the loss in 123-keV γ rays the extent of diffusion could be determined. The drop in the 123-keV counting rate, $N_{123}^0 - N_{123}'$, was due to actual loss of activity due to the annealing; and N_{123}' , the counting rate of the 123-keV γ rays after annealing, is proportional to the strength of the source. The large drop in 14.4-keV rate was due to attenuation of the 14.4-keV γ rays by the host, and hence R , defined

²¹ The tests for Co and Ni were made on known portions of activity (≈ 1 mCi) as measured in our standard counter geometry. The test was made on basic solutions of the activity using dilute rubenic acid (dithio-oxamide) in alcohol as a reagent, and the results compared with identical tests made simultaneously on standard solutions of Co and Ni. These tests were sensitive to 0.2 μg of total Co and Ni. The test for Fe was a visual examination of the acid solution of the activity after it had been concentrated (a 25 mCi lot was reduced to ≈ 0.2 ml by evaporation); 10 ppm Fe in acid gives an unmistakable yellow color.

TABLE I. Source preparation data, results of anneal, estimates of impurity concentrations, and zero-field linewidths.

Source	Annealing temperature (°C)	Annealing time (h)	Annealing atmosphere	Cleanup	mCi in source	Area of source (mm ²)	R [Eq. (1)] (μg/mCi)	Original impurity ^a [Eq. (4)]	D (mm)	Impurity introduced ^b (at. ppm)	Host impurity ^c (at. ppm)	Total magnetic impurity ^d (at. ppm)	Other impurity ^e (at. ppm)	Linewidth ^f (Room temp./4°K) (mm/sec)
V-1	1220	5	H ₂ +Ar	HNO ₃ +HF	1.38	20	0.69	0.22	1.4 × 10 ⁻²	90 (150, 50)	400	500	3000 O ₂	0.49 0.44
V-2	1120	4	H ₂ +Ar	HCl	0.88	27	0.96	0.48	0.16 × 10 ⁻²	700 (4000, 100)	400	1000	100 Si <3000 O ₂	0.37 0.41
Nb	1450 1050	1½ 4	H ₂ +He vacuum	H ₂ O	1.63	7	0.77	0.22	0.9 × 10 ⁻²	500 (1000, 200)	0 (30)	500	300 Zr <1000 W	0.34 0.34
Ta	1550 1050	3 18	H ₂ +He vacuum	HF	0.49	5	0.26	0.22	0.6 × 10 ⁻²	400 (1000, 150)	30	400	300 Nb	0.34 0.35
Pt	1110	0.83	4.5	0.57	0.6 ⁱ	0.17 × 10 ⁻²	5000 (20 000, 1000)	...	~6000	10 ⁸ to 10 ⁴ Ag <1000 Ta	...
W	1650 1080	3½ 16	H ₂ vacuum	ε	0.95	28	0.50	0.22	0.24 × 10 ⁻²	300 (500, 200)	20	300	None	0.31 0.29
Mo high-purity	1550 1050	1½ 3	H ₂ vacuum	H ₂ O	0.46	16	0.40	0.22	4.0 × 10 ⁻²	15 (30, 10)	10 (70)	50	None	0.31 0.33
Mo stock	1470 1050	3½ 48	H ₂ vacuum	HCl	1.13	27	0.94	0.35	0.2 × 10 ⁻²	600 (2000, 200)	900	1500	400 Si	0.30 0.33
Au mono-crystal	810	½	H ₂ +Ar	HCl	0.83	27	0.2	0.35	0.76 × 10 ⁻²	150 (200, 100)	50 (150)	200	None	0.30 0.35
Au foil	~810	...	H ₂	HCl	1.05	36	^h 0.6 ⁱ	800 (4000, 200)	0 (150)	1000	100 Cu	...
Ag mono-crystal	910	2	H ₂ +Ar	HNO ₃	0.30	35	0.26	0.22	4.0 × 10 ⁻²	5 (9, 3)	2 (12)	10	None	0.29 0.32
Cu mono-crystal	910	1	H ₂ +Ar	HCl	1.28	27	0.70	0.35	0.5 × 10 ⁻²	200 (300, 160)	3 (9)	200	None	0.32 0.32
Cu stock	925	...	H ₂ +Ar	HCl	12	27	0.38	0.6 ⁱ	1.7 × 10 ⁻²	1000 (3000, 400)	0 (9)	1000	None	0.31 0.29
Rh	1370 1050	3 3	H ₂ vacuum	Hot H ₂ SO ₄ aqua regia, HF	0.68	30	0.82	0.48	0.4 × 10 ⁻²	200 (1000, 40)	120	300	100 Pt	0.30 0.30

^a Our spot-test estimate of the magnetic impurity concentration in the activity as obtained from supplier.

^b Estimated magnetic impurity concentration (C) due to radioactive solution [see Eq. (5)]. The numbers in parentheses indicate the range of possible values. The uncertainty is due primarily to inaccuracy in the spot-test determination of contaminants in activity.

^c Magnetic impurity concentration (Fe, Co, and Ni) for host materials before adding activity. Upper limits are in parentheses.

^d Our best estimate of total magnetic (Fe+Co+Ni) contaminants.

^e Other contaminants in excess of 100 ppm as reported spectroscopically (or by O₂-gas analysis of a similarly heat-treated sample).

^f Observed linewidths at room temperature (listed first) and 4°K against a K₂Fe(CN)₆·3H₂O absorber.

^g Data were taken on this source which was only washed with H₂O. The source was then etched with HF+HNO₃, removing 20% of the 14.4-keV counting rate, and data were taken again, with identical results.

^h The foil was 0.00014 in. thick, and the activity is diffused uniformly through it since both sides have identical counting rates.

ⁱ The activity used for these old sources was not spot tested; however, the supplier called it "carrier-free" and it showed no yellow iron color. Thus, the figure quoted is somewhat arbitrary and has been assigned a factor-of-3 error.

below, is a measure of the diffusion depth since μ_x , the γ -ray attenuation coefficient, is known.²²

$$R = (N_{14}'/N_{123}')/(N_{14}^0/N_{123}^0), \quad (1)$$

where the primes refer to the counting rates after annealing.

Autoradiographs, conveniently done using Polaroid 4- × 5-in. ASA 3000 film, were made to determine the uniformity of the deposit and the effective surface area of the source.

Thus, if R and C , the amount of contaminants per unit area on the surface are known, and the impurity concentration $C(y)$ at a distance y from the surface is assumed to be $C(0)e^{-a^2y^2}$, then (1) the average diffusion depth D , and (2) C , the average atomic impurity concentration from which a 14.4-keV γ ray originates, can be calculated. $C(0)$ is the concentration at the surface after annealing. To make the calculations, a is determined from the definition

$$R = \int_0^\infty e^{-a^2y^2} e^{-\mu_x y} dy / \int_0^\infty e^{-a^2y^2} dy, \quad (2)$$

where $\int_0^\infty e^{-a^2y^2} dy = \pi^{1/2}/2a$, and $C(0)$, in atomic ppm, is determined from

$$C(\mu\text{g}/\text{cm}^2) = (\pi^{1/2}/2a)(M/M')\rho'C(0), \quad (3)$$

where M is the atomic weight of the impurity and M' and ρ' are the atomic weight and density of the host. Then D and C are found from their definitions

$$D = \int_0^\infty y e^{-a^2y^2} dy / \int_0^\infty e^{-a^2y^2} dy, \quad (4)$$

and

$$C = \int_0^\infty C(y) e^{-a^2y^2} e^{-\mu_x y} dy / \int_0^\infty e^{-a^2y^2} e^{-\mu_x y} dy. \quad (5)$$

It might be noted that $C/C(0)$ varies from 1 to 0.7 depending on the relative values of μ_x and a . For Eqs. (4) and (5) to be valid it is required that the sources be thick compared to D , a condition well satisfied in all cases except the Au foil. Columns lettered (a) through (f) of Table I represent measurements and best estimates of the concentration of impurities for the sources employed. The individual columns are further identified in the footnotes to the table.

Also reported in Table I are values of the resonance linewidth at two temperatures. A source having approximately the natural linewidth would show a linewidth of 0.29 mm/sec against this $\text{K}_4\text{Fe}(\text{CN})_6 \cdot 3\text{H}_2\text{O}$ absorber. Linewidths in excess of this value may be due to impurities or strains causing quadrupole splitting, due to nonequivalence of impurity sites, or due to spin coupling between impurities. Throughout this paper

²² The attenuation coefficients for the 14.4-keV γ rays were obtained from *Handbook of Chemistry and Physics*, edited by C. D. Hodgman (The Chemical Rubber Publishing Company, Cleveland, 1960), p. 2665.

experimental linewidths refer to the observed full width at half-maximum (FWHM) of the resonance overlays of source and absorber.

EXPERIMENTAL RESULTS

The Co^{57} impurity has a half-life of 270 days, and 90% decays by electron capture and gamma transitions to Fe^{57m} , the first excited state. Fe^{57m} is the Mössbauer state with a mean lifetime of 0.14 μsec , a magnetic moment $\mu_1 = -0.155$ nuclear magnetons, and a spin $I_1 = \frac{3}{2}$. The $M1$ gamma transition of energy $E_\gamma = 14.37$ keV leads to the Fe^{57} ground state whose magnetic moment $\mu_0 = +0.0903$ nuclear magnetons and whose spin $I_0 = \frac{1}{2}$. Owing to the selection rules, the energy spectrum of the γ rays emitted in a particular direction \mathbf{r} , relative to \mathbf{H}_{eff} , the effective magnetic field at the Fe^{57} nucleus, should consist of six lines whose amplitudes obey the ratio $3:\beta:1:1:\beta:3$. In general β varies from 0 to 4 depending on \mathbf{r} .^{23,24} The lines of intensity β correspond to the transitions from the excited state to the ground state with $\Delta m = 0$ where m is the magnetic quantum number for each state.

From the magnetic moments of these nuclear states it is possible to determine H_{eff} from the Mössbauer hyperfine spectrum. H_{eff} is, in detail, the average magnetic field at the nucleus over a time comparable to the hyperfine resolution time (the precession time of the nuclear spin in the magnetic field). With a magnetic field H applied to the sample,

$$\mathbf{H}_{\text{eff}} = \mathbf{H} + \mathbf{H}_i, \quad (6)$$

which defines \mathbf{H}_i , an internal magnetic field characteristic of Fe^{57} in its environment.

For the sources discussed in this paper, it was found that the $\Delta m = 0$ lines in the Mössbauer spectra were not present, which indicates that \mathbf{H}_{eff} is parallel (positive) or antiparallel (negative) to \mathbf{H} .²⁴ From polarization measurements the signs of H_{eff} in Cu, Pd, and Au were determined at low temperatures and are consistent with a negative H_i . For the remainder of the sources, it was found indirectly that H_i was also negative,²⁵ except for V, Nb, and Ta, where $H_i \approx 0$. These determinations of

²³ S. S. Hanna, R. S. Preston, and J. Heberle, *Proceedings of the Second International Conference on the Mössbauer Effect* (John Wiley & Sons, Inc., New York, 1962) p. 88; R. S. Preston, S. S. Hanna, and J. Heberle, *Phys. Rev.* **128**, 2207 (1962).

²⁴ H. Frauenfelder, D. E. Nagle, R. D. Taylor, D. R. F. Cochran, and W. M. Visscher, *Phys. Rev.* **126**, 1065 (1962).

²⁵ At room temperature $H_{\text{eff}} \approx H$ for all sources studied; furthermore, polarization measurements on Fe in Cu show H_{eff} to be positive with respect to H . The data for temperature behavior of H_{eff} for Fe in Mo in a constant $H = 62$ kOe demonstrates how a negative H_i is implied. At 200°K, $H_{\text{eff}} = +58$ kOe, the same size as found for Fe in Cu. As the temperature is lowered H_{eff} decreases smoothly until at about 8°K $H_{\text{eff}} = 0$ indicating $H + H_i = 0$. At still lower temperatures $|H_{\text{eff}}|$ increases smoothly; at 0.45°K $H_{\text{eff}} = -51$ kOe and $-H_i > H$. These observations give an increasing $|H_i|$ with decreasing temperature (a reasonable assumption for paramagnetic behavior). The "crossover" temperature where $-H_i = H$, ($H_{\text{eff}} = 0$) for $H = 62$ kOe was observed directly for the following sources: 4°K for Fe in W; 5°K for Fe in Rh; and 8°K for Fe in Mo.

the sign of the effective field are in agreement with some recent Mössbauer polarization measurements on Cu, Au, Rh, and Mo containing Fe.²⁶ In the absence of an external field none of these sources showed a hyperfine splitting, indicating no spontaneous magnetic ordering down to the lowest temperatures studied; however, some sources showed some temperature-independent line broadening (see Table I) for $H=0$.

Data Analysis

The known Mössbauer spectrum of Fe⁵⁷ in Fe was used for velocity calibration of the spectrometer. Generally, a narrow single-line copper source external to the cryostat and an enriched Fe absorber were used. A very slight linear dependence of the calibration upon the applied field H was noted and was taken into account. An Fe source and a ferrocyanide absorber were occasionally used for calibration and were found to agree with the iron absorber calibrations. Owing to demagnetizing effects, use of iron foils for calibration could lead to a small systematic error of possibly 1%. For the data reported here we have used a value of 52.3 kOe for the separation of the two innermost lines of the hyperfine spectrum of Fe⁵⁷ reported by Hanna *et al.*²³; their stated uncertainty was about 1%.

Owing to possible error in the manufacturer's calibration of the solenoid, an additional systematic error of 0.5% may exist. An intercomparison of several superconducting solenoids in this laboratory has shown agreement among the calibrations to within less than this error.

The Mössbauer spectra of each source were determined with the ferrocyanide absorber at a variety of temperatures and applied fields. For a well-resolved hyperfine spectrum H_{eff} was deduced directly from the peak locations of the outer pair of lines and the drive calibration. For those spectra where $H_{\text{eff}} \lesssim 30$ kOe, corrections to the peak locations were necessary. For $H_{\text{eff}} \sim 0$ kOe, where no hyperfine structure was resolved, H_{eff} was determined from line broadening.

The overlap of source-absorber lines both having natural linewidths would give ideally a linewidth of ~ 6 kOe. Even for ideal polarized source spectra (3:0:1:1:0:3), the inner lines and the overlap tails of the outer lines affect the peak locations appreciably for $H_{\text{eff}} \lesssim 10$ kOe. The linewidth of the ferrocyanide absorber was about double the natural linewidth and the source emission lines were somewhat broader than ideal so that corrections to the peak locations are necessary for $H \lesssim 30$ kOe.

The actual corrections were determined from computed theoretical spectra assuming a Lorentzian line shape in the source and in the absorber and 3:0:1:1:0:3 intensities for the emission lines located at the proper relative velocities. The calculated curves depend somewhat upon the linewidth of the absorber relative

to the source; experimental linewidths were used in the calculations. The actual shape of the calculated spectra was generally found to match observed spectra quite closely both in zero field and in an applied field.

In those cases where the outer peaks were not resolved, H_{eff} was determined from line broadening and comparison with the computed spectra. Accuracy of this method requires a careful definition and determination of the background, a precise knowledge of the linewidth appropriate to no applied field, and a consistent definition of the average peak height of the complex spectrum. Usually H_{eff} was determined both from apparent splitting and from broadening whenever the outer peaks were partially resolved and agreement to within 0.8 kOe was always found.

In a few instances H_{eff} could be determined from the splitting of the inner pair of lines as well as the outer pair of lines. The splitting found for the inner lines was that expected using H_{eff} from the outer lines and the known level splittings.²³

As mentioned earlier, errors due to small nonlinearities in the Doppler drive tend to cancel out in our data analysis; furthermore, the drive was found to be linear for most of these experiments.

The "standard error" for the results shown subsequently allows for statistical errors and for systematic errors (absolute magnet and drive calibration errors and small uncertainties in obtaining values of H_{eff} when the spectra are not resolved) in determining H_i ; uncertainties associated with determining H and T are less than 1% and are not shown.

Simple Magnetic Behavior

In the analysis of the hyperfine spectra, it is always assumed that the applied field acts directly on the nuclear moments of the Fe⁵⁷ impurity; additional contributions to H_{eff} are defined by Eq. (6) to be H_i . Thus, the simplest case one might encounter is one where $H_i=0$ at all temperatures and applied fields. Such was essentially the case for Fe impurities in three elements which have an electron concentration $n=5$.

Vanadium, Niobium, and Tantalum, $n=5$

The magnetic behavior of dilute Fe⁵⁷ impurities in V, in Nb, and in Ta was almost identical. These elements, located in the Va column of the periodic table all become superconductors at temperatures accessible in this study. The applied fields were always greater than the critical fields for measurements on these sources.

Two vanadium sources were studied, V-1 and V-2, with nominal magnetic impurity concentrations of 500 and 1000 atomic ppm, respectively. The measured value of H_{eff} for these two samples was within 1 kOe of the applied field for $T=0.5$ to 35°K and $H=6$ to 62 kOe. This small difference, defined as H_i , was always found to be positive; however, the combined systematic and

²⁶ N. Blum and L. Grodzins, Phys. Rev. **136**, A133 (1964).

experimental errors assigned to these measurements allow that $H_i=0$. The data are plotted in Fig. 2(a) and will be discussed later.

Source V-1 had a very broad line (see Table I) at all temperatures studied. The spectrum of this source had been measured at room temperature after the initial reduction in H_2 and Ar; a single line of width FWHM of 0.34 mm/sec was obtained against the ferrocyanide absorber. Further annealing seemed to be dictated by the R ratio, and the broad line V-1 resulted. Source V-2 was made in an effort to produce a narrow line source by repeating only the preliminary treatment of V-1. The attempt was only partially successful. Source V-1 was quite brittle compared to the starting material. These changes are probably related to the O_2 , N_2 , and H_2 content of the V. The high affinity of V for O_2 combined with the increased gas porosity of the quartz furnace tube at elevated temperatures during the final vacuum cooldown of the source yielded an O_2 content more than three times that stated by the manufacturer for the starting material.

Detailed study of V-2 at 0.49 and 1.11°K for $H=62.0$ kOe showed that the outer pair of resolved hyperfine lines had the same (broad) linewidth as was observed in no field.

The niobium source had a nominal magnetic impurity concentration of 500 ppm. The H_{eff} for this source was consistently greater than the applied field for $T=1.1$ to 200°K and $H=6$ to 62 kOe. Data are presented in Fig. 2(b). An average linewidth of $0.32_3 \pm 0.005$ mm/sec for the well-resolved outer pair of hyperfine lines for this source in 62.0 kOe at 1.1, 4.0, and 200°K is in good agreement with the $H=0$ linewidth of 0.34 mm/sec quoted in Table I.

The tantalum source used in this investigation had a nominal magnetic impurity concentration of 400 ppm. The H_{eff} for this source was consistently greater than the applied field for $T=0.5$ to 3.96°K and $H=20$ to 62 kOe, as shown in Fig. 2(c). At 0.5°K and 62.0 kOe a linewidth of 0.35 mm/sec was measured for the outer pair of lines compared to 0.29 mm/sec for a source having natural linewidth. The slight broadening found for both Nb and Ta is also probably related to the presence of dissolved O_2 , H_2 , and N_2 in the sources. Line narrowing of the hyperfine components has been reported for the very broad line of Fe^{57} in Ti when subjected to large applied fields¹⁸; it is generally thought that the broadening in Ti is chiefly due to quadrupole splitting of the Fe^{57} in a hexagonal environment. As indicated above, the (somewhat) broad lines of cubic V, Nb, and Ta remain broad in high external fields.

Figure 2 indicates without exception a trend toward positive H_i . At least, for Nb and Ta, there is also a trend for H_i to increase with H ; the slope of a straight line through the origin and through the data at 62 kOe; for the three sources increase from 0.007 for V to 0.011 for Nb to 0.015 for Ta. Such a behavior bears a striking

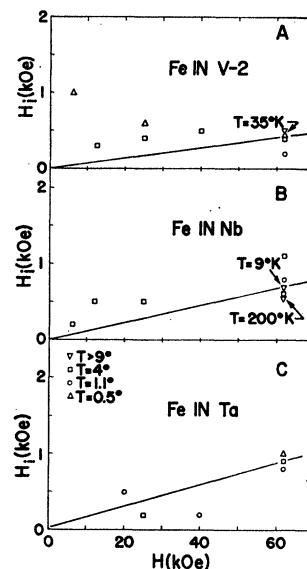


FIG. 2. Vanadium, niobium, and tantalum data. The standard error is 1 kOe.

resemblance to the Knight shift of the pure metals.²⁷ The shift reported for V and Nb is 0.0055 and 0.0085, respectively,²⁷ and 0.011 for Ta.²⁸ The relative behavior of H_i at 62 kOe for the three sources is believed to be significant in spite of the assigned error of 1–2% and ± 1 kOe to a particular measurement.

Because H_i is so small and is independent of temperature, we conclude that there is no localized moment associated with dilute Fe impurities in V, Nb, or Ta.

Phenomenological Theory

In an earlier investigation¹ the behavior of H_i for a very dilute Fe^{57} impurity in Pd was explained in terms of a simple paramagnetic model. The internal field determined from the Mössbauer hyperfine spectra and Eq. (6) was taken to be proportional to the long-term time average of the electronic spin component in the direction of H .^{1,11} That is,

$$H_i = H_{sat} \langle J_z \rangle / J, \quad (7a)$$

where J_z is the component of the spin J of the system in the direction of H , and H_{sat} is H_i when the spin system is completely polarized.

The simple paramagnetic model also assumed that the field acting on every impurity nucleus is H plus an induced field arising from a free quantum-mechanical spin system localized about the Fe impurity with total spin J in the applied field. Thus

$$H_i = H_{sat} B_J(x) \begin{cases} \rightarrow H_{sat} & \text{for } x \geq 4 \\ \rightarrow H_{sat}(J+1)x/3J & \text{as } x \rightarrow 0, \end{cases} \quad (7b)$$

²⁷ See, for example, a review by W. D. Knight, in *Solid State Physics*, edited by F. Seitz and D. Turnbull (Academic Press Inc., New York, 1956), Vol. 2, p. 93.

²⁸ T. J. Rowland, *Progr. Mater. Sci.* **9**, 1 (1961).

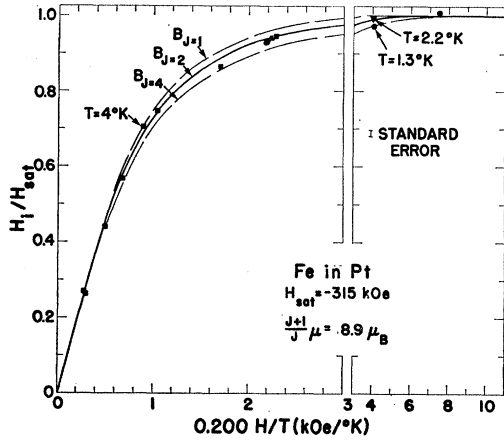


Fig. 3. Platinum data. The standard error is ± 3 kOe. The theoretical curves for $1 \leq J \leq 4$ are within the error of these data.

where $B_J(x)$ is the Brillouin function for spin J with $x = \mu H/kT$, μ is magnetic moment of the spin system, and k is Boltzmann's constant.

In this work where $H > 30$ kOe, and where the hyperfine structure was well resolved, each component of the hyperfine spectra was at least as narrow as the zero-field line for all sources at all temperatures studied. Thus, we find, experimentally, all Fe⁵⁷ impurities have identical magnetic environs, a requirement in order for the above model to be valid.

Platinum and Palladium, $n = 10$

The platinum source used in this investigation had a nominal magnetic impurity concentration of 6000 atomic ppm. The data reduced in terms of the paramagnetic model are presented in Fig. 3. The source, located in the center of a small 50-kOe solenoid, was directly immersed in the He⁴ bath in a manner similar to that reported for Pd.¹ H_{eff} was determined over the range 1.3 to 4°K at $H = 6$ to 49 kOe from spectra which were always well resolved because of the large value of the localized moment μ together with the large value of H_{sat} . The best fit of the experimental data to the Brillouin function for $J = 2$ gives $H_{\text{sat}} = -315$ kOe and $(J+1)\mu/3Jk = 0.200$. The latter is equivalent to $(J+1)\mu/J = 8.9\mu_B$. Also shown in Fig. 3 are the B_J curves for $J = 1$ and $J = 4$; as is evident, this method is not a very sensitive way to determine J . Using $J = 2$, these results indicate a localized moment on the Fe $\mu = 6.0\mu_B$ and a gyromagnetic ratio $g = \mu/J\mu_B = 3$. The present data confirm the low-field measurements¹ for the moment of Fe in Pt.

Complete data for Fe in Pd were reported earlier,¹ and the results will only be summarized here for comparison. As discussed before, the Brillouin behavior adequately described the data, and the best fit indicated that $H_{\text{sat}} = -295 \pm 3$ kOe, $J = 13/2 \pm \frac{3}{2}$, and $\mu = 12.6 \pm 0.4\mu_B$. A value of 1.94 ± 0.4 for g results. No estimate of the purity of the source was given; however, one can

imply that the Co concentration was less than 1000 atomic ppm from data of Bozorth *et al.*,³ who measured a Co_{0.001}Pd_{0.999} to be ferromagnetic below 7°K. Ferromagnetism was not observed at 1.5°K for the source used by Craig *et al.*¹

Expanded Phenomenological Theory

Upon the investigation of very dilute Fe impurities in other cubic metals, it was found that the simple paramagnetic theory was not adequate to describe the experimental data. The data can be approximately described even at the lowest temperatures by the addition of a single parameter which arises if the theory is expanded in a rather simple way to account for a *hypothetical* interaction of the localized spin system with an assumed field for the host.

The supposed interaction of the localized spin \mathbf{J} with the host will be considered in terms of a randomly fluctuating vector field $\mathbf{s}(t)$ of the host which couples to \mathbf{J} . Assuming that the thermal relaxation times and the precession times for \mathbf{J} are short compared to the average period p of $\mathbf{s}(t)$, then the average of the component of \mathbf{J} along the field at the atom over the hyperfine resolution time τ_0 is

$$\langle \mathbf{J} \rangle_{\tau_0} = J \left\{ \frac{(\mu \mathbf{H} + k \mathbf{s}(t) \cdot \mathbf{J})}{|\mu \mathbf{H} + k \mathbf{s}(t)|} \right\} \times B_J \left\{ \frac{|\mu \mathbf{H} + k \mathbf{s}(t)|}{kT} \right\}_{\tau_0}. \quad (8)$$

If we further assume that $p \gg \tau_0$, and that $\mathbf{s}(t)$ has (in °K) a magnitude s independent of time, temperature, and magnetic field, Eq. (8) can be computed as the average over all possible orientations of \mathbf{s} . In general, Eq. (7a) becomes

$$H_i(J, T, \mu H, s) = H_{\text{sat}} \langle J \rangle_{\tau_0} / J. \quad (9)$$

It is perhaps instructive to note the behavior of H_i for several limiting cases in this modified theory.

$$\begin{aligned} H_i(J, T, \mu H, s) &\rightarrow H_{\text{sat}} B_J(\mu H/kT) && \text{as } (T/s) \rightarrow \infty, \\ &\rightarrow \frac{2}{3} \mu H_{\text{sat}} / ks && \text{as } (T/s) \rightarrow 0 \\ &\rightarrow H_{\text{sat}} && \text{for } (\mu H/ks) < 0.6, \\ &&& \text{and } (\mu H/kT) \rightarrow \infty. \end{aligned} \quad (10)$$

We have found it convenient to present $H_i(J, T, \mu H, s)$ in two different ways. The first is appropriate when s is small and the behavior of the internal field approximates Brillouin behavior; for a given J , a family of (H_i/H_{sat}) curves will be presented as a function of $(J+1)\mu H/3JkT$ and the parameter s/T . When s is large compared to T , a second (but equivalent) way of presenting the theory and data is introduced in order to emphasize the limiting low-temperature behavior of H_i . In this case a family of $(ksH_i/\mu H H_{\text{sat}})$ curves will be presented as a function of $\ln\{3JT/(J+1)s\}$ and the parameter $\mu H/ks$. $\mu H/ks$ is typically less than 1 for large s , and $\alpha = -(H_i/H)$ is closely approximated by a function of T only.¹²

Tungsten and Molybdenum, $n=6$

Figure 4 presents the experimental data for our tungsten source with a nominal magnetic impurity concentration of 300 atomic ppm. The data have been analyzed in terms of the expanded theory and are presented in the way for approximate Brillouin behavior. The solid line in Fig. 4 is $B_J(\mu H/kT)$, and data taken at $T \geq 4^\circ\text{K}$ should lie, within the experimental error, on this line if the theory is valid. For data taken at lower temperatures the behavior deviates from the Brillouin curve. The long-dashed curve is the theoretical behavior of data taken at 1.1°K , and the short-dashed curve is the theoretical behavior of data taken at 0.51°K assuming $(J+1)s/J=2.1^\circ\text{K}$. The best fit of the experimental data indicates that for Fe in W, $H_{\text{sat}} = -76.0$ kOe and that $(J+1)\mu/J=4.33\mu_B$.

Figure 5 presents the experimental data for our molybdenum sources of high-purity Mo and stock Mo with nominal magnetic impurity concentrations of 50 and 1500 ppm, respectively. The data have been analyzed in a way similar to that for the tungsten data. Since s is again about 2°K , the data for $T \geq 4^\circ\text{K}$ should lie on the Brillouin curve. From the fit to the data, we deduce $H_{\text{sat}} = -114.5$ kOe, $(J+1)\mu/J=3.75\mu_B$ and $(J+1)s/J=2.6^\circ\text{K}$ for Fe in Mo.

These two Mo sources, as well as the W source before and after a deep acid etch, showed anomalous behavior at low temperatures ($T \lesssim 4^\circ\text{K}$) and low field ($H \lesssim 30$ kOe). Each of the anomalous spectra had the same character—an added resonance strength near the center of the hyperfine spectra. The spectra did not resemble computed $3:\beta:1:1:\beta:3$ spectra with $0 < \beta < 4$, the admissible range of β . Therefore, the anomalous central resonance cannot be simply expanded in terms of a single internal field polarized in the usual or any other direction. For either Mo source at $T < 4^\circ\text{K}$ and $H = 6.3$ kOe, the added central resonance corresponded to perhaps 20% of the total resonance; this percentage

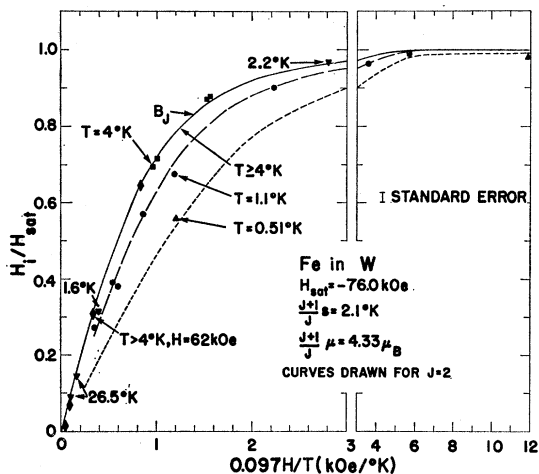


Fig. 4. Tungsten data. The standard error is ± 1 kOe. The theoretical curves for $1 \leq J \leq 3$ are within the error of these data.

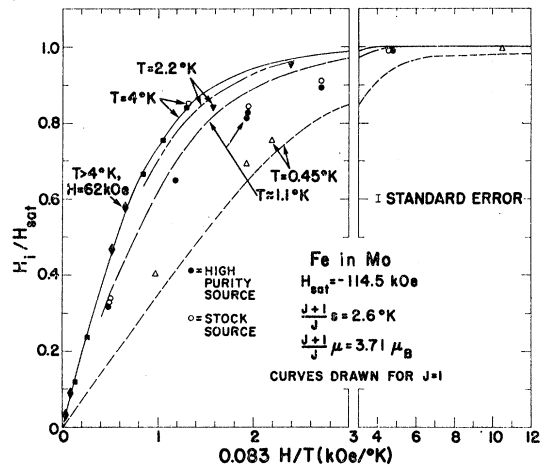


Fig. 5. Molybdenum data. The standard error is ± 1 kOe. The theoretical curves for $J \leq 1$ are within the error of these data. Stock-source data labeled as taken at 1.1°K were actually taken at 1.2°K , so they should lie higher than the high-purity data, as they do. $(J+1)s/J=4^\circ\text{K}$ would provide a good fit at 1 and 2°K , but worse at 0.5°K .

decreased at increased applied fields and disappeared in the neighborhood of $H = 30$ kOe. In addition, a broadening of the outer pair of hyperfine lines was noted at low T for $H < 35$ kOe. At $T = 1.1^\circ\text{K}$ and $H = 25$ kOe (the minimum field for well-resolved spectra), the linewidth for Fe in Mo was found to be more than 1.5 times that found at $H = 62$ kOe or $H = 0$; this corresponded to almost a threefold increase in the source linewidth. Crude estimates on data taken at 1.1°K and 12 kOe gave this same degree of broadening. In spite of the interesting anomalies mentioned, reasonable values of H_i were obtained for all H and T from the outer lines and are included in Figs. 4 and 5.

The value for the localized moment of Fe in Mo is in disagreement with the low value reported earlier,¹ which was based on preliminary measurements using the Mössbauer technique. The cause of the discrepancy is fully understood; measurements made at 4°K and 30 kOe yield $H_{\text{eff}} \approx -33$ kOe (Fig. 5). Craig *et al.*¹ obtained essentially the same splitting; however, they assumed H_{eff} to be positive and to correspond directly to the applied field and deduced the localized moment was $< 0.2\mu_B$.²⁹

Gold, Silver, and Copper, $n=11$

Figure 6 shows the experimental data for our single-crystal gold source with a nominal magnetic impurity concentration of 200 atomic ppm. The data have been analyzed by the expanded theory for approximate Brillouin behavior of the internal field. At 4 and 2.2°K , the theory could represent the data quite well; however,

²⁹ Measurements in Ref. 1 were made only between 1.5 and 4°K for $H < 30$ kOe using a very broad Fe-Ti absorber. The erroneous conclusion that $\mu < 0.2\mu_B$ for Fe in Cu and in Rh stems from the absence of a large hyperfine splitting and an absence of a H/T dependence in this range.

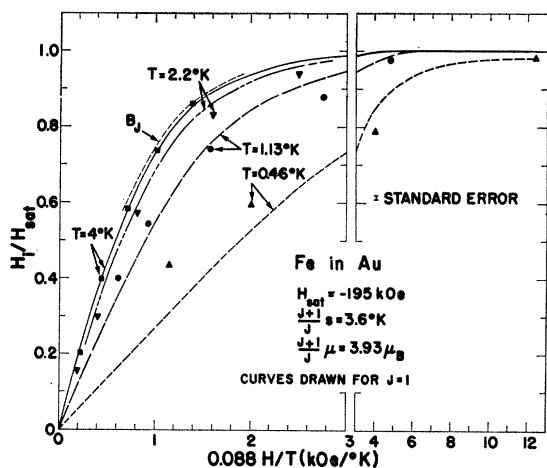


FIG. 6. Gold data. The standard error is ± 1 kOe. The theoretical curves for $J \leq 1$ are within the error of these data.

at lower temperatures it appears that even the functional form predicted by the modified theory is not proper. This suggests that the deviations from pure paramagnetism are brought about by some other mechanism or, at least, that the simplifying assumption that s is independent of H and T is not valid. The theoretical curves given in the figure are determined using the parameters listed. In spite of slight deviations from ideal Brillouin behavior at 4°K , obtaining data above 4°K seemed unnecessary; furthermore, adequate stabilization of temperatures above 4°K for the long counting times required for this very weak source was difficult.

A second gold source¹⁶ made from foil had a nominal magnetic impurity concentration of 1000 ppm. The experimental data could be fitted as in Fig. 6, using the same parameters except for H_{sat} . $H_{\text{sat}} = -173$ kOe was required. The quality of the fit was about the same as that in Fig. 6. This is the only case where two well-

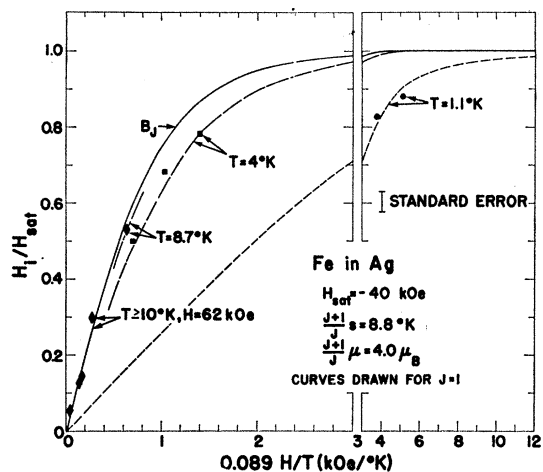


FIG. 7. Silver data. The standard error is ± 1 kOe. The theoretical curves for $\frac{1}{2} \leq J \leq 3$ are within the error of these data.

behaved sources of the same host material gave different experimental results.

The experimental data for our silver single-crystal source with a nominal magnetic impurity concentration of 10 ppm are presented in Fig. 7 and have been analyzed in a manner similar to that used for Fe in Au. The solid solubility of Co and Fe in Ag has been reported³⁰ to be less than 13 ppm. That we were able to diffuse a few ppm Co⁵⁷ into Ag at 910°C and obtain a narrow line source from which meaningful measurements could be made points out one of the big advantages of the Mössbauer technique—an ability to work with extremely dilute systems. The data fall, within experimental error, on the theoretical curves shown for the parameters given in Fig. 7. Significant deviations from B_J behavior are shown to exist below 10°K , but may be accounted for by the modified theory using the value of s shown. This is the first case presented where little information could be obtained along the B_J curve beyond its linear region; to do so would require much larger magnetic fields than are available so that substantial spin alignment could be effected at temperatures above 20°K .

Whenever s is still larger, the advantages of a plot of the type of Fig. 7 showing classical spin paramagnetism behavior are less apparent and an alternative presentation will be used. The same data for Fe in Ag are given in Fig. 8 in order to show that the same information can be obtained from the new presentation. The limiting behavior of H_i at low T for a given H is more clearly indicated.

In Fig. 9, are presented the experimental data for Fe in Cu reduced in the manner of Fig. 8. One source was a copper single crystal having a nominal magnetic impurity concentration of 200 ppm; a second polycrystalline source contained a nominal 1000 ppm magnetic impurities. The latter source was used in a previous investigation¹²; those data as well as new data for the source are included in Fig. 9. Two other polycrystalline sources having an estimated 40 and 5000 ppm magnetic impurity concentration confirmed the

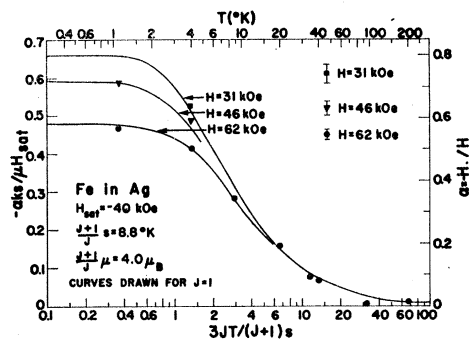


FIG. 8. Silver data. This figure is equivalent to Fig. 7. The vertical scale is 0.825α and the horizontal scaling is $0.34 T$.

³⁰ M. Hansen, *Constitution of Binary Alloys* (McGraw-Hill Book Company, Inc., New York, 1958), 2nd ed.

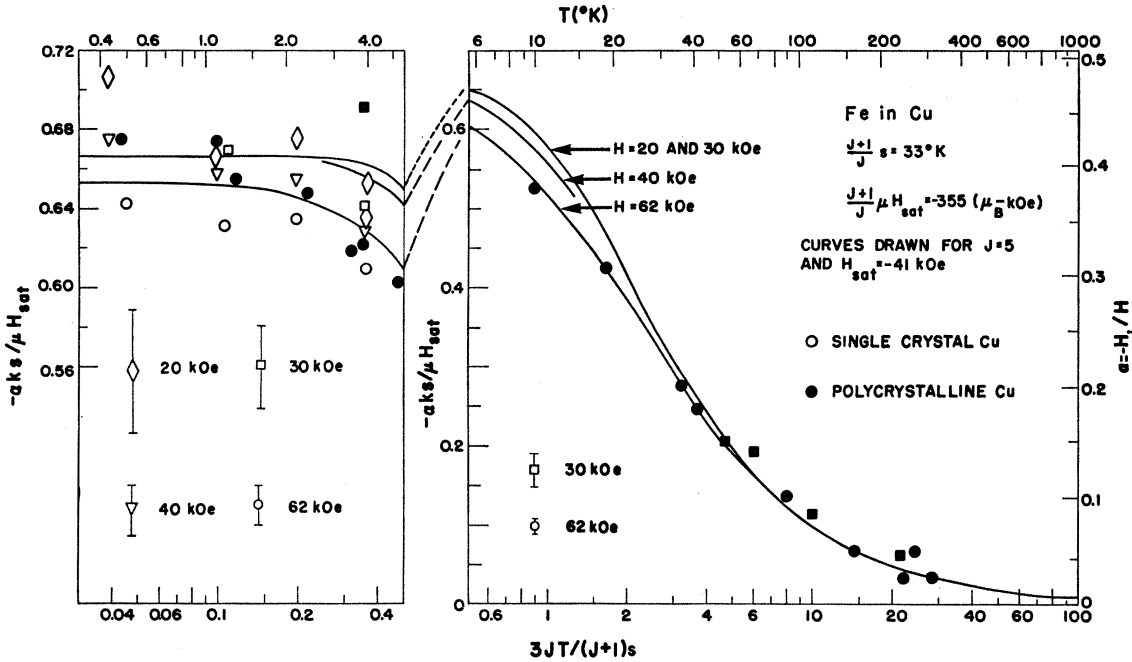


FIG. 9. Copper data. The standard error is ± 0.5 kOe. The vertical scaling is 1.38α and the horizontal scaling is $0.091 T$. Because sufficient fields are not available a precise determination of $H_{\text{sat}}(J+1)\mu/J$ only is possible; H_{sat} and $(J+1)\mu/J$, individually, are not accurately known. The choice of $J=5$ is somewhat arbitrary.

value of $\alpha = -H_i/H$ at 4°K at high fields.¹² There appears to be a slight difference in the H_i determined for each of the two sources reported in Fig. 9 for temperatures below 4°K; however, this difference is only slightly outside the combined experimental error. The data for the single crystal source strongly suggest a slight trend in the value of α with H , as is accounted for in the modified theory. A more stringent test of the theory would require precise measurements at substantially higher fields than were available. Furthermore, at higher fields a better determination of H_{sat} and μ would be possible.

Rhodium, $n=9$

In Fig. 10 we present the experimental data for our rhodium source with a nominal magnetic impurity concentration of 300 atomic ppm. The best fit provided by the expanded theory shows some systematic deviations, especially at higher temperatures. Although the data lie within experimental error of the theoretical curves, the deviations suggest a behavior more complicated than that specified by our treatment of Eq. (8).

In Table II we summarize for each source studied the parameters derived from the best fit of the experimental data and list the probable errors associated with the determination of each of these parameters.

Temperature and Chemical Shifts

As a bonus to our study on localized moments, information on the temperature shifts^{14,31} and chemical

³¹ B. D. Josephson, Phys. Rev. Letters 4, 341 (1960).

(isomeric) shifts¹⁵ was obtained. These data are presented in Fig. 11 in terms of the fractional energy shift from the 14.4-keV γ ray of an Fe in Fe source at 296°K. Because this investigation was not a systematic study of the shift as a function of temperature, some points on this graph correspond to only one datum while others represent the average of ten or more determinations. The standard error $\pm 0.5 \times 10^{-13}$ corresponds to the reproducibility of a determination and is therefore more characteristic of a single datum. Most of the shifts were determined in the presence of a high

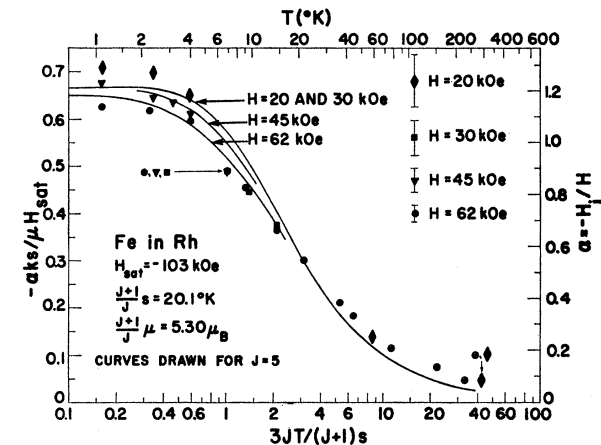


FIG. 10. Rhodium data. The standard error shown is ± 2 kOe, but data taken above 20°K have only ± 1 kOe error. The vertical scaling is 0.55α and the horizontal scaling is $0.149 T$. The poor quality of the fit makes the choice of $J=5$ somewhat arbitrary.

TABLE II. Summary of results.

Source	n	$\frac{J+1}{J}S$ (°K)	$-\frac{(J+1)}{J}\mu H_{\text{sat}}$ (μ_B -kOe)	$-H_{\text{sat}}$ (kOe)	$\frac{J+1}{J}\mu$ (μ_B) ^a	$\frac{\Delta\epsilon}{\epsilon}\times 10^{13}$ ($T \leq 4^\circ\text{K}$)	$\frac{\Delta\epsilon}{\epsilon}\times 10^{13}$ ($T = 296^\circ\text{K}$)
V	5	...	0	...	0	-1.4 ± 0.5	-5.5 ± 0.5
Nb	5	...	0	...	0	4.6 ± 0.5	-0.5 ± 0.5
Ta	5	...	0	...	0	6.1 ± 0.5	1.1 ± 0.5
Pt	10	1 ± 1	2820 ± 60	315 ± 6	8.94 ± 0.09	17.0 ± 0.6^c	12.0 ± 0.6^c
Pd	10	0	4300 ± 90^b	295 ± 9^b	14.5 ± 0.3^b	11.5 ± 0.6^c	6.8 ± 0.6^c
W	6	2.1 ± 0.2	330 ± 3	76 ± 1	4.33 ± 0.04	9.3 ± 0.5	5.5 ± 0.5
Mo	6	2.6 ± 1	425 ± 4	115 ± 1	3.71 ± 0.04	6.1 ± 0.5	2.0 ± 0.5
Au	11	3.6 ± 1.4	765 ± 8	195 ± 2	3.93 ± 0.04	26.7 ± 0.5	21.3 ± 0.5
Ag	11	8.8 ± 0.4	160 ± 8	40 ± 6	4.0 ± 0.6	22.4 ± 0.5	17.5 ± 0.5
Cu	11	33 ± 3	355 ± 20	82^{+80}_{-40}	4.4^{+4}_{-2}	11.8 ± 0.5	7.6 ± 0.5
Rh	9	20 ± 3	545 ± 60	103^{+100}_{-50}	5.3^{+5}_{-3}	8.2 ± 0.5	3.8 ± 0.5

^a Notice that $\mu = [(J+1)\mu/J] - g\mu_B$.

^b Taken from Ref. 1.

^c Taken from Ref. 32; room temperature stated to be 298°K.

magnetic field (12 to 62 kOe) generally from the location of the center of gravity of the hyperfine spectra as determined from the resolved outer pair of lines. These shifts showed no systematic deviations from the corresponding shifts measured in zero field. No distinc-

tion is made in Fig. 11 between data obtained in zero field and in an applied field. The solid curves shown are those calculated from the Debye theory for the best fit θ stated on the figure.^{14,32} For completeness on this graph, data for platinum were taken from Ref. 32. Their data were taken using the same platinum source as was used in determining the localized moment. The results of the shift determinations for $T \leq 4^\circ$ and for $T = 296^\circ\text{K}$ are tabulated in Table II.³³

DISCUSSION

Contributions to the Internal Field

The Mössbauer hyperfine spectrum is a measure of the internal magnetic field H_i at the nucleus according to Eq. (6). The origins of this field have been discussed by Watson and Freeman.¹¹ They show that the dominant contributions to H_i are due to the Fermi contact interaction; therefore, H_i will be assumed proportional to the polarization of the electron spin density at the Fe⁵⁷ nucleus in this discussion. Since the electron density at the nucleus is primarily conduction electrons and s electrons, the major contributions arise from their polarization. These polarization mechanisms are briefly described below.

(1) The applied field polarizes the conduction electrons as in the description of the Knight shift.²⁷ The contribution to the internal field from the ordinary Knight shift is generally positive (in the direction of H), proportional to H , independent of the temperature, and is of the order of 0 to 2% of H . Such a small contribution to H_i can be important only in the cases of V, Nb, and Ta. At higher temperatures than were studied, where the paramagnetic contribution becomes small, such effects might be observed with the other hosts.

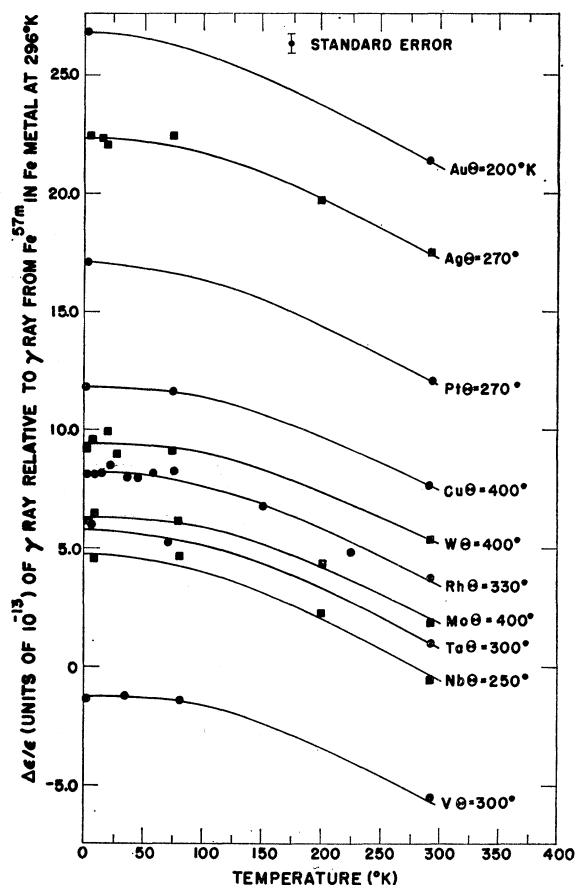


FIG. 11. Chemical (isomer) and temperature-shift data of Fe⁵⁷ in various hosts. The theoretical curves from the Debye theory of solids are shown for the θ 's listed at the right. Positive $\Delta\epsilon$ means higher γ -ray energy in the source.

³² W. A. Steyert and R. D. Taylor, Phys. Rev. 134, A716 (1964).

³³ For comparison purposes the fraction energy shift for the Pd source used by Craig *et al.* (Ref. 1) is $11.5 \pm 0.6 \times 10^{-13}$ at 4°K and $6.8 \pm 0.6 \times 10^{-13}$ at 298°K as determined by Steyert and Taylor (Ref. 32).

Some experimental evidence has been presented which suggests that a contribution to the internal field for Fe in V, Nb, or Ta exists which fulfills the above criteria for the Knight shift. In fact, the values of H_i/H are in semiquantitative agreement with known values of the Knight shift for the pure host metals. This surprising agreement may be fortuitous, for it is known that the changes of the nmr Knight shift for a given dilute, nonmagnetic impurity in a variety of nonmagnetic metallic hosts are small (compared to our shift of Fe in various hosts). No pertinent Knight shift data for Fe⁵⁷ or Co⁵⁹ were available.

(2) The outer unpaired electronic spins of the Fe⁵⁷ impurity ($\sim 3d$ in character) are polarized by the extra-atomic fields. In turn, these unpaired spins polarize the spins of the s electrons. Because the density of the s electrons is finite at the impurity nucleus, a small polarization of the s electrons results in a large H_i , which in the case of Fe⁵⁷ is opposite in sign to the field caused directly by the polarization of the spins of the $3d$ shell.³⁴ The fact that the field from the s electrons is expected to be proportional to the $3d$ polarization leads us to Eq. (7a), $H_i = H_{\text{sat}} \langle J_z \rangle / J$. This relation assumes that the nuclear spin-electron coupling is so weak that the nuclear moment does not follow the quickly changing electronic spin system, but is only affected by the time average of the spin system. This point of view is reasonable in light of the estimated lifetime of the localized states on Fe in Cu of 10^{-15} sec,⁵ while the nuclear spin requires more than 10^{-8} sec to precess. From near infrared data on Ni_{0.07}Au_{0.93} the estimated lifetime of the localized state at the Ni site is 2×10^{-15} sec.³⁵

The Localized Magnetic State

The nature of the $3d$ electrons of the Fe⁵⁷ impurity in nonmagnetic metallic hosts has been investigated by several workers in the past.^{2,4-8} Friedel⁴ and Wolff⁶ have visualized a virtual bound state: A conduction electron moves along, falls into the well formed by the impurity potential, orbits as a $3d$ electron, and then continues on its way. Anderson⁵ considers the impurity state as a local $3d$ state admixed with the states of the conduction band and shows by a self-consistent calculation that the states are magnetic when they are sufficiently narrow and the states corresponding to different spins lie on different sides of the Fermi energy.

Clogston *et al.*² have analyzed the magnetic susceptibility data of 1% Fe in the $4d$ metals and alloys in terms of localized magnetic moments and found that the moments were a function of the average electron concentration outside the last closed shell to a good

approximation. The similarity of the $3d$, $4d$, and $5d$ bands leads to the similarity of the moments of Fe⁵⁷ in V, Nb, and Ta; Pd and Pt; Mo and W; and Cu, Ag, and Au reported above.

It should be pointed out that only a part of the observed moment is localized on the impurity atom. Experimental evidence of this comes from neutron diffraction and nuclear magnetic resonance and will be discussed later. Thus as Freeman³⁶ points out, we should not expect $H_{\text{sat}} = -125\mu$, as might be expected if all the spin were on the Fe,¹¹ but instead H_{sat} should have a magnitude something less than that, but negative, as is observed. Similarly Clogston predicts $1.5\mu_B$ on Fe impurities in Mo and a total of $1.1\mu_B$ on the neighboring Mo.³⁷

Deviations from Pure Paramagnetic Behavior

If the localized moments are well-isolated, pure paramagnetic behavior is expected. For pure paramagnetic behavior, the spins are free and the evaluation of $\langle J_z \rangle / J$ is simple.

$$\frac{\langle J_z \rangle}{J} = \sum_{J_z} J_z e^{J_z x} / J (\sum_{J_z} e^{J_z x}) = B_J(x), \quad (11)$$

where $x = \mu H / kT$.

In the higher temperature domain, the results reported here are compatible with the idea of free spins. However, at low temperatures, all localized moments except those in Pd and Pt show deviations from a free spin behavior. This, in itself, is not unexpected; at some low enough temperature, the strength of interactions between impurity atoms will become comparable to T , and thus perturb the free spin behavior. We shall show that the impurity-impurity interactions are *not* the cause of the observed low-temperature deviations, suggest other possible causes, and elaborate on the meaning of the randomizing parameter utilized in the data analysis.

Deviations from free spin behavior in magnetic susceptibility theory are usually analyzed in terms of the relation

$$\langle J_z \rangle / J \cong (J+1)\mu H / 3Jk(T-\theta) \quad (12)$$

for small $\mu H / (T-\theta)$. Making a simple calculation of the Curie-Weiss constant θ assuming that the magnetic ions have a concentration c and are randomly distributed in a nonmagnetic matrix with a coordination number Z and that only nearest-neighbor interactions of strength J exist, we find that $\theta = Zc/2k$. More detailed calculations³⁸ result in $\theta = (Zc/2k)f(kT/J)$; again, θ is dependent on c . However, at very low impurity concentrations, nearest-neighbor interactions play only a

³⁴ Reference 11 shows that the direct interaction between the polarized d shell and the nucleus is small, as is H_i associated with the $4s$ wave functions which are admixed to the $3d$ band.

³⁵ B. Caroli, preprint quoted by G. J. van den Berg, in *Progress in Low Temperature Physics*, edited by C. J. Gorter (North-Holland Publishing Company, Amsterdam, 1964), Vol. 4, p. 259.

³⁶ A. J. Freeman, Phys. Rev. **130**, 888 (1963).

³⁷ A. M. Clogston, Phys. Rev. **136**, A1417 (1964).

³⁸ H. Sato, A. Arrott, and R. Kikuchi, J. Phys. Chem. Solids **10**, 19 (1959).

small role (if the concentration of impurities is 100 ppm and the number of nearest neighbors is $Z=8$, then only one impurity in 10^3 will have another impurity for a nearest neighbor). Instead, the long-range Ruderman-Kittel interaction will be the predominant impurity-impurity coupling mechanism.

The Ruderman-Kittel interaction is an impurity-electron-impurity coupling.³⁹ The coupling varies as $(\cos 2k_F r)/r^3$ for long impurity-impurity distances (r), where k_F is the wave number of an electron at the Fermi surface. The situation is now much harder to calculate, and long- and short-range cooperative effects are expected. However, one can easily see that the average r varies as $c^{-1/3}$ and the average two-body interaction strength is proportional to c . If such interactions were causing the low-temperature deviations, it would be surprising that the two Mo sources listed in Table I could have such similar behavior as shown in Fig. 5, since their impurity concentrations differ by a factor of better than 10. Furthermore, the two copper sources (Table I, Fig. 8) had the same α (thus s) to within an experimental error of $\pm 1.6\%$. Although the gold foil source and the pure single-crystal source listed in Table I had different values of H_{sat} , they did have the same s and μ values.

Other possible causes for the deviation of the observations from the expected behavior which are not impurity-concentration-dependent are as follows:

(1) As the temperature is lowered, there is an increase in the electron spin-lattice relaxation time. This results in a breakdown of Eq. (7a) if the nuclear spin partially follows the fluctuating electronic spin when the relaxation time becomes comparable to the hyperfine resolution time $\cong 10^{-7}$ sec. In this case the Mössbauer hyperfine lines become broadened, the spectrum becomes more complicated to interpret, and for sufficiently long relaxation times the pattern may even become a composite of several discrete fields. The latter such effects have been observed in a dilute paramagnetic material by Obenshain *et al.*⁴⁰ and by Campbell *et al.*,⁴¹ and a theory has been developed for such materials for no applied field by Afanas'ev and Kagan.⁴² The anomalous patterns observed at low H and low T for Mo and W may be related to long electron spin-lattice relaxation times although such long relaxation times are unlikely in metals. Furthermore, long relaxation times can hardly account for the behavior of Fe in Cu where the deviations are very large at temperatures as high as 20°K, while at all temperatures

the component lines of the hyperfine spectrum are narrow and are consistent with the expected 3:0:1:1:0:3 spectra to as low as 0.5°K and $H=20$ kOe.

(2) It has been suggested that Overhauser spin density waves in the conduction electrons are acting as a perturbing influence on the impurity spins.¹³ Their calculation assuming spiral waves gives results in agreement with previously published data on Fe in Cu.¹²

(3) There is the possibility of localized hot spots at the emitting nucleus resulting from the recoil energy of the preceding 123-keV γ ray. However, research on temperature spikes indicates that the temperature of the nucleus will return to the temperature of the host lattice within 10^{-11} sec.⁴³ Since this is 4 orders of magnitude smaller than the nuclear lifetime, the heating effect should be negligible.

The phenomenological model used to analyze our results (see experimental results), considers a randomizing host-impurity coupling \mathbf{s} , which may be impurity spin-host lattice or impurity spin-host spin in nature, or may have some other origin. In this model, \mathbf{s} was assumed to be completely random and so a spherical average in Eq. (8) was used. Calculations based on traveling \mathbf{s} waves of constant magnitude and longitudinal and transverse as well as spiral \mathbf{s} waves were made. Generally, the data were adequately described by both the spiral and spherical averages, but the latter was used because it appears to be a more reasonable physical assumption. We chose a model for comparison purposes which can be applied for all H and T , and adds only one new parameter, the constant s . It is s which gives a measure of the deviation from free spin behavior, as does the Curie-Weiss constant θ of Eq. (12). From the figures it can be seen that this model gives a reasonable fit to the results, except for Mo (Fig. 5) and for Au at 0.46 and 1.1°K (Fig. 6). In the tabulation of results (Table II), the measured quantities with large assigned errors are those which are sensitive to the details of the randomizing assumptions, and should be accepted only to the extent that one believes there is some validity in these assumptions.

White and Clogston have calculated the temperature dependence of a localized moment for an orbital singlet state.⁴⁴ Assuming that the Fermi level bisects the unmagnetized state, the theory could be done analytically and they found that below some critical temperature T_c , depending on the level width and the Coulomb repulsion between electrons localized in the state, the moment was nonzero and proportional to $[1 - (T/T_c)^2]^{1/2}$. This dependence is not consistent with the deviations from a constant moment in our Fe in

³⁹ M. W. Klein and R. Brout, *Phys. Rev.* **132**, 2412 (1963).

⁴⁰ F. E. Obenshain, L. D. Roberts, C. F. Coleman, D. W. Forester, and J. O. Thomson, *Proceedings of the Ninth International Conference on Low Temperature Physics*, Columbus, Ohio (to be published).

⁴¹ L. Campbell, F. de S. Barros, and S. DeBenedetti, *Bull. Am. Phys. Soc.* **9**, 634 (1964).

⁴² A. M. Afanas'ev and Yu. Kagan, *Zh. Eksperim. i Teor. Fiz.* **45**, 1660 (1963) [English transl.: *Soviet Phys.—JETP* **18**, 1139 (1964)].

⁴³ F. Seitz and J. S. Koehler, *Solid State Physics*, edited by F. Seitz and D. Turnbull (Academic Press Inc., New York, 1956), Vol. 2, p. 355.

⁴⁴ J. A. White and A. M. Clogston, *J. Appl. Phys.* **34**, 1187 (1963).

Cu data, for example. The statistical mechanics of localized states in a d -band metal also indicate that the magnetization deviates from simple paramagnetic behavior.⁷

An analysis, analogous to Eq. (12), has been used for the magnetic Mössbauer data for dilute Fe in Cu with some success¹⁶; however, such an approach was found inadequate for other sources reported here.

Comparison with Other Experimental Data

Several other physical effects also provide information concerning magnetic impurities in the transition metals. A brief explanation of these effects and a comparison of the available experimental data with the results of this investigation can now be given. In this comparison it must be recalled that the Mössbauer effect measures the total moment and spin associated with the impurity, not just those on the Fe⁵⁷ itself, as pointed out by Freeman.³⁶

Neutron Scattering and Nuclear Magnetic Resonance

Neutron-scattering data in conjunction with magnetization measurements provide information on the magnetic moments associated with individual atoms. For dilute magnetic impurities, the alloys are disordered so that ferromagnetic diffuse scattering measurements are required and it is not possible to work with less than about 1 at.-%. An investigation on two reasonably dilute systems has been carried out by Cable, Wollan, and Koehler.⁴⁵ Using Pd_{0.97}Fe_{0.03} and Pd_{0.93}Fe_{0.07}, they found $3.0 \pm 0.2 \mu_B$ on the Fe in both cases. Their analysis assumed that all Pd atoms had the same moment and was $0.15 \pm 0.01 \mu_B$ for the 3 at.-% Fe sample and $0.27 \pm 0.02 \mu_B$ for the 7 at.-% Fe sample.

When the nuclear magnetic moment of a nucleus is known, it is theoretically possible to determine the magnetic field at the nucleus by nuclear magnetic resonance (nmr). Ehara has made nmr measurements on Co⁵⁹ in the same CoPd alloys used by Bozorth *et al.* in an investigation of their susceptibility.⁴⁶ Since the resonance is nearly independent of concentration from 0.5 to 2.0% Co and is almost the same as for pure Co, Ehara concludes that the magnetic moment of a Co atom in these alloys is the same as that associated with Co in pure Co, $1.7 \mu_B$. He then accounts for the excess moment associated with the Co atoms from the susceptibility study by postulating that Pd atoms which have two or three Co nearest neighbors have $0.6 \mu_B$ and those Pd atoms with fewer Co nearest neighbors have smaller moments.

⁴⁵ J. W. Cable, E. O. Wollan, and W. C. Koehler, *J. Appl. Phys.* **34**, 1189 (1963).

⁴⁶ Shaw Ehara, *J. Phys. Soc. Japan* **19**, 1313 (1964); R. M. Bozorth, P. A. Wolff, D. D. Davis, V. B. Compton, and J. H. Wernick, *Phys. Rev.* **122**, 1157 (1961).

Specific Heat

Any magnetic impurity present in a nonmagnetic host will contribute an entropy of $k \ln(2J+1)$, where J is the total spin associated with the impurity, not just that on the impurity atom. In order to determine J , the entropy of the pure nonmagnetic host is subtracted from that of the dilute magnetic alloy; but unless the impurities do not interact or do not change the entropy of the lattice, conduction electrons, or other contributing mechanisms, this difference will not equal $k \ln(2J+1)$ per impurity. If one neglects these difficulties for 0.05, 0.1, and 0.2 at.-% Fe in Cu, a spin of $\frac{1}{2}$ is found associated with each Fe from specific heat measurements from 0.4°K.⁴⁷ An independent investigation on 0.1 at.-% Fe in Cu also indicates $J = \frac{1}{2}$ per Fe and the specific heat anomaly for Fe in Au has been observed.⁴⁸

Electron Transport Properties

Anomalies in the electrical resistance have been observed in dilute magnetic alloys by Sarachik *et al.* for 1 at.-% Fe in Mo-Nb and Mo-Re alloys; by Knook for 5 to 1000 at. ppm Fe in Cu; by Coles for 0.10, 0.50, and 0.85 at.-% Fe in Rh; and by MacDonald *et al.* for 20, 60, and 200 at. ppm Fe in Au.⁴⁹ An explanation of the behavior of these alloys by Kondo is based on the s - d interaction model of the localized state.⁴⁹ The calculated spin scattering of conduction electrons is linearly dependent on the concentration and logarithmically dependent on the temperature in agreement with the experimental results.

The magnetic impurity, acting as a spin-dependent scattering center for conduction electrons, will also cause "giant" thermoelectric powers. Such powers have been observed for Fe in Au, Ag, Cu, Pt, and other hosts, but no quantitative interpretation has been made.⁵⁰

Superconducting Transition Temperature

If iron exhibits a local moment in a superconductor it may dramatically decrease the superconducting transition temperature (T_c). For instance, T_c in Mo_{0.8}Re_{0.2} is decreased 22°K/at.-% Fe.⁵¹ The discovery

⁴⁷ J. P. Franck, F. D. Manchester, and D. L. Martin, *Proc. Roy. Soc. (London)* **A263**, 494 (1961).

⁴⁸ G. J. van den Berg, in *Progress in Low Temperature Physics*, edited by C. J. Gorter (North-Holland Publishing Company, Amsterdam, 1964), Vol. 4, p. 240.

⁴⁹ M. P. Sarachik, E. Corenzwit, and L. D. Longinotti, *Phys. Rev.* **135**, A1041 (1964); B. Knook, thesis, University of Leiden, 1962 (unpublished); R. B. Coles, *Phys. Letters* **8**, 243 (1964); D. K. C. MacDonald, W. B. Pearson, and I. M. Templeton, *Proc. Roy. Soc. (London)* **266**, 161 (1962); and Jun Kondo, *Progr. Theoret. Phys. (Kyoto)* **32**, 37 (1964).

⁵⁰ This problem is reviewed by D. K. C. MacDonald, in *Thermoelectricity: An Introduction to the Principles* (John Wiley & Sons, Inc., New York, 1962), pp. 31-36 and pp. 69-83. Experimental results on resistance anomalies are also discussed.

⁵¹ B. T. Matthias, M. Peter, H. J. Williams, A. M. Clogston, E. Corenzwit, and R. C. Sherwood, *Phys. Rev. Letters* **5**, 542 (1960).

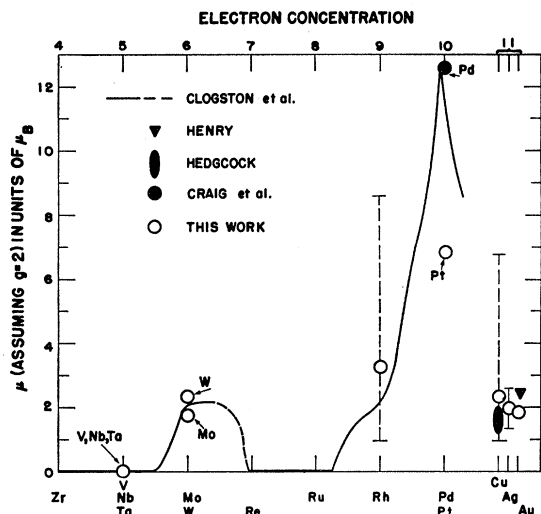


FIG. 12. The curve represents the results of susceptibility measurements of 1% Fe in the 4-*d* transition metals and the 5-*d* metal Re as well as the alloys Nb-Mo, Mo-Re, Ru-Rh, Rh-Pd, and Pd-Ag. (Clogston *et al.*) The abscissa scale shows the value of the electron concentration of the host metals. Henry and Hedgcock results are from susceptibility measurements, and the Craig *et al.* results are from Mössbauer measurements.

of superconductivity was made in Mo⁵² and W⁵³ only after much care was taken to obtain Fe free material. Where Fe has no local moment in a superconductor, the addition of Fe has only a small effect; for instance in Nb, T_c is decreased by only 0.22°K/at. % Fe.⁵⁴ In V, Fe decreases T_c by 1.1°K/at. %.⁵⁵ This is probably associated with changes in the electron concentration, which changes the density of states at the Fermi surface, an important parameter in the BCS theory of superconductivity. These results are consistent with our measurements and susceptibility measurements, i.e., no local moment exists for Fe in V or Nb, but one does exist for Fe in Mo and W. Our results suggest that small amounts of Fe in Ta would not alter T_c very much (Fe is not very soluble in Ta, which makes such measurements difficult).

Other Mössbauer Data

Borg *et al.*⁵⁶ measured the splitting of Mössbauer γ rays in Fe and Au alloys of compositions such that the alloy was ferromagnetic. Calculating H_{eff} from their hyperfine splitting values and extrapolating along the magnetization curve to $T=0^\circ\text{K}$ gives us values of H_{eff} versus composition. This value H_{eff} in zero external field can be equated to H_{sat} except for demagnetization effects. Plotting these results and extrapolating to

⁵² T. H. Geballe, B. T. Matthias, E. Corenzwit, and G. W. Hull, Jr., Phys. Rev. Letters **8**, 313 (1962).

⁵³ J. W. Gibson and R. A. Hein, Phys. Rev. Letters **12**, 688 (1964).

⁵⁴ T. H. Geballe, Rev. Mod. Phys. **36**, 134 (1964).

⁵⁵ J. Muller, Helv. Phys. Acta **32**, 141 (1959).

⁵⁶ R. J. Borg, R. Booth, and C. E. Violet, Phys. Rev. Letters **11**, 464 (1963).

0% Fe gives $|H_{sat}| = 225$ kOe compared to our value of -195 kOe.

Blum *et al.*¹⁸ have reported an absence of an internal field for 1% Fe⁵⁷ in Ti and Sc from measurements of H_{eff} for absorbers in fields up to 110 kOe at temperatures over the range 1.5 to 300°K, implying the absence of a localized moment. Large negative contributions to the hyperfine field were reported for 1% Fe⁵⁷ in Mo and in Rh and for a Co⁵⁷ in Cu source, indicative of the presence of a localized moment. Co⁵⁷ in Au is in substantial agreement with the present results.⁵⁷

Magnetic Susceptibility

The contribution to the susceptibility χ (in emu/gm) of a material due to magnetic impurities is

$$\chi' = \eta \mu \langle J_z \rangle / JH, \quad (13)$$

where η is the number of impurity atoms per gram and the magnetic moment μ and the spin J are associated with the impurity and its surroundings, not just the impurity atom. χ' is determined experimentally by subtracting the susceptibility of the pure host from the measured χ . Since only rather high concentrations of impurities provide accurate results, the form of $\langle J_z \rangle / J$ given in Eq. (12) must be used in Eq. (13). Thus,

$$\chi' = \eta \left(\frac{J+1}{3J} \right) \frac{\mu^2}{k(T-\theta)}. \quad (14)$$

Equation (7a) used in the Mössbauer technique and Eq. (13) are quite generally valid and form the basis for the following comparisons. Figure 12 shows the values of μ obtained from our measurements compared to values of μ obtained from the susceptibility data. The Clogston *et al.*² results represent their reported values. The Henry⁵⁸ and Hedgcock⁵⁹ values are obtained by our fitting their higher temperature susceptibility measurements to Eq. (14) to obtain $[(J+1)/J]^{1/2} \mu$. Not shown is a value of $4.8 \mu_B$ for 13.4 at. % Fe in Pt⁶⁰ and $2.45 \mu_B$ for 0.6 at. % Fe in Au.⁶¹ Childs *et al.*⁶² conclude that the addition of small amounts of Fe to V results in no unpaired spins ($\mu=0$). The choice of $g=2$ for comparison purposes is arbitrary, but is permitted by the $(J+1)\mu/J$ values and J limits reported (Figs. 3-8).

⁵⁷ A. J. Freeman (private communication).

⁵⁸ W. E. Henry, Phys. Rev. Letters **11**, 468 (1963).

⁵⁹ F. T. Hedgcock, Phys. Rev. **104**, 1564 (1956). Because data are not available between 30 and 300°K, the μ we deduce has the uncertainty shown by the size of the point in Fig. 12.

⁶⁰ J. Crangle, J. Phys. Radium **20**, 435 (1959). This μ is low because at this high concentration Fe atoms must share magnetized Pt neighbors; thus $\mu/(\text{Fe atom})$ is lowered.

⁶¹ Sato *et al.* (Ref. 38) interpret the susceptibility results of A. R. Kaufmann, S. T. Pan, and J. R. Clark, Rev. Mod. Phys. **17**, 87 (1945) to obtain $[(J+1)/J]^{1/2} \mu = 3.3 \mu_B$ for 0.6 at. % Fe in Au. If $g=2$, this implies $\mu = 2.45 \mu_B$.

⁶² B. G. Childs, W. E. Gardner, and J. Penfold, Phil. Mag. **8**, 419 (1963). When the high concentration of Fe ($\approx 23\%$) makes the electron concentration greater than 5.6, the spins unpair ($\mu \neq 0$).

CONCLUSIONS

The Mössbauer effect is a useful tool in obtaining information about impurity states in metals. Among the advantages of the method are the following: Concentration of impurities can be very low, and very small samples are practicable, a precise knowledge of the concentration is not required to determine the localized moment, homogeneity and equivalence of impurity sites may be implied from linewidths and the hyperfine spectrum, the magnitude and sign of the effective field is readily determined, the internal field and the saturation field may be determined over a wide range of H/T values allowing (in some cases) an independent determination of J and μ , the spin polarization at the Fe site is deduced directly (rather than from a change of some measured property of the host lattice) and any transition arising from a spontaneous magnetization should be readily apparent in the hyperfine spectrum.

There is good agreement between Mössbauer and susceptibility values of the impurity state moment μ . The agreement where intercomparison is possible, then, lends confidence to the Mössbauer measurements

where they are the only ones available (i.e., in Ag and Ta, where Fe is almost insoluble). When higher magnetic fields are available, we hope to obtain better values for μ in Ag, Cu, and Rh by obtaining measurements of H_i closer to H_{sat} .

The Mössbauer results are also in qualitative agreement with impurity studies using measurements of electron transport (electrical resistance and thermoelectric power). Transport measurements can also be made using very dilute impurities at low temperatures; however, quantitative intercomparison awaits a better understanding of the mechanisms involved. If a randomizing host-impurity coupling does exist, as suggested, it can be expected to have a large influence on the low-temperature electron-impurity scattering and hence the transport properties.

ACKNOWLEDGMENTS

We gratefully acknowledge the necessary high-temperature anneals done for us by D. T. Eash and the assistance given by D. R. F. Cochran with the radiochemistry.